Raman signal enhancement for gas detection using a dual near–concentric cavities group

Yifan Ren (任一凡)[1], Dewang Yang (杨德旺)[2], Yingxin Sun (孙颖欣)[1], Jiaxuan Xu (许家旋)[1], Shuofang Liu (刘硕芳)[1], and Yuee Chen (陈月娥)[1*]

[1] Key Laboratory for Microstructural Material Physics of Hebei Province, School of Science, Yanshan University, Qinhuangdao 066004, China

[2] College of Ocean Science and Engineering, Shandong University of Science and Technology, Qingdao 266590, China

*Corresponding author: 552001140@qq.com

Effective methods are urgently required to optimize Raman spectroscopy technology to ameliorate its low detection sensitivity. Here, we superposed two near-concentric cavities to develop a dual near-concentric cavities group (DNCCG) to assess its effect on gas Raman signal intensity, signal-to-noise ratio (SNR), and limit of detection (LOD). The results showed that DNCCG generally had higher CO_2 Raman signal intensity than the sum of two near-concentric cavities. Meanwhile, the noise intensity of DNCCG was not enhanced by the superposition of near-concentric cavities. Accordingly, DNCCG increased the SNR. The LOD for CO_2 was 24.6 parts per million. DNCCG could be an effective method to improve the detection capability of trace gases and broaden the dynamic detection range, which might aid the future development of innovative technology for multicomponent gas detection.

Keywords: Raman spectroscopy; gas detection; sensitivity; dual near-concentric cavities group.
DOI: 10.3788/COL202422.051202

1. Introduction

The continuously increasing concentration of trace gases in the atmosphere is one of the major contributors to the elevated global surface temperature[1]. Real-time and accurate monitoring of trace gas concentrations is of utmost importance to adapt and mitigate ongoing global warming. Raman spectroscopy technology is a fast, efficient, and nondestructive method for trace gas detection. It has the advantages of simultaneous detection of multicomponents, a large detection concentration range, being a simple device, and *in situ* detection. Based on the above advantages, this technology has been applied to hazardous materials detection[2,3], gas composition analysis[4–6], environmental monitoring[6–8], and medical diagnosis[9,10]. However, the signal intensity of spontaneous Raman scattering is weak and susceptible to fluorescence interference[11], leading to low detection sensitivity. This limits the further application of the technology. Therefore, it is of utmost importance to develop new strategies to optimize traditional Raman spectroscopy technology to further ameliorate its low detection sensitivity.

Multiple reflection cavities can improve detection sensitivity by increasing the effective optical path length[12–15]. In addition, this technology can make the low-power laser realize the power amplification in the out cavity, achieving the effect of a high-power laser[16] and avoiding the technical difficulties of building a high-power laser. Therefore, it has been widely applied to *in situ* gas component detection. In 1974, Ill *et al.*[17] applied the plano–concave cavity to improve Raman spectral sensitivity, and the experimental gain was 93 times. This was the first application of the multiple reflection cavity to improve the Raman spectral sensitivity. In recent years, many studies have improved the multiple reflection cavities to further enhance the detection sensitivity of Raman spectroscopy. For example, Utsav *et al.*[18] improved the multiple-pass cavity with a multiple-pass optical cell[19] and built a concentric cavity that enhanced the Raman signal intensity and the signal-to-noise ratio (SNR). Moreover, previous studies also found that increasing the reflection times of the incident beam can enhance the ray density and luminous flux at the center of the multiple reflection cavity. Some methods used this ray distribution to further enhance the signal intensity of multiple reflection cavities. For example, Yang *et al.*[20] replaced the traditional concentric cavity with a near-concentric cavity by slightly adjusting the angle on one side of the spherical mirror. This shift increased the reflections of the incident beam, enhancing the signal intensity and SNR by more than 70 times and decreasing the limit of detection (LOD) of CO_2 to 97 ppm (parts per million). Liu *et al.*[21] further improved the near-concentric cavity by adding a mirror to the center of the optical cavity, building a gas Raman spectrum measurement system based on a folded near-concentric cavity. The optimized

near-concentric cavity increased the ray density at the center of the multiple reflection cavity, which increased the SNR by 1.4 times and achieved the LOD of 66 ppm and 11 ppm for CO_2 and CH_4, respectively. Consequently, improving the multiple reflection cavity can enhance the signal intensity and SNR, decrease the gas LOD, and increase the detection sensitivity of gas Raman spectroscopy. However, the detection sensitivity of trace gas in previous findings is still limited by the lower signal detection capability and detection range. Thus, effective methods are urgently required to further enhance the gas Raman signal detection capability, improve detection sensitivity, and obtain a more extensive dynamic detection range.

To this end, the present study proposed and developed a gas Raman spectroscopy system based on a dual near-concentric cavities group (DNCCG). To understand the ray distribution in the DNCCG, TracePro software was used to simulate ray tracing and luminous flux before and after the superposition of the near-concentric cavities. To further verify the simulation results, we built a gas Raman spectroscopy enhancement system based on DNCCG to evaluate its detection capability. The aim of this study was to (1) simulate the ray distribution in DNCCG, and perform ray tracing to determine the reflections of the incident beam and the luminous flux at the coincidence point of the beam waists, (2) evaluate the effect of DNCCG on the Raman signal intensity and SNR of CO_2, and (3) determine the effect of DNCCG on the LOD of CO_2. Our findings could improve the multiple reflection cavity-enhanced gas Raman spectroscopy technology and provide scientific insights into the development of trace gas monitoring technologies.

2. Simulation and Experiment

2.1. Simulation of near-concentric cavities and DNCCG

In this paper, through the simulation of TracePro software, the luminous flux of two near-concentric cavities at the beam waists and the change of the luminous flux of DNCCG at the coincidence point of the beam waists after the superposition of two near-concentric cavities are analyzed (see Fig. 1). Based on this, the Raman signal enhancement effect of the system is evaluated.

The laser beam used in the simulation is set as Gaussian distribution, the X and Y radii of the beam waist at $1/e^2$ are 0.3 mm,
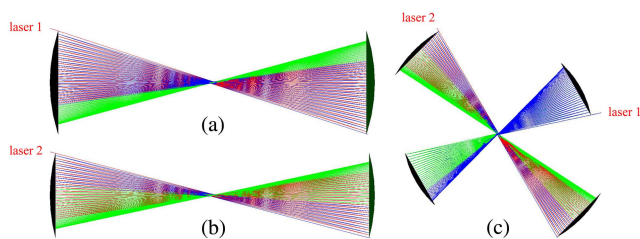
and the power of laser 1 is 0.5 W and that of laser 2 is 1.0 W. A concentric cavity is created by positioning two spherical mirrors at a distance of 4 times the focal length. The incident angle of the light is adjusted to align its distribution with the mode of the concentric cavity. Subsequently, fine adjustments are made to one side of the concentric cavity's mirror to match the light distribution with the mode of the near-concentric cavity. Some specific parameters and methods are as follows. Briefly, the reflectivity of the four mirrors is set to 99% at 532 nm. Two concave mirrors with a diameter of 25.4 mm and a focal length of 20 mm, with a spacing of 80 mm, are aligned and then the right mirror is rotated clockwise by 0.006° to obtain near-concentric cavity A, as shown in Fig. 1(a). Two concave mirrors with a diameter of 25.4 mm and a focal length of 25 mm, with a spacing of 100 mm, are aligned and then the right mirror is rotated clockwise by 0.007° to obtain near-concentric cavity B, as shown in Fig. 1(b).

2.2. Experiment design

The device diagram of the gas Raman spectroscopy system of DNCCG built in this paper is shown in Fig. 2. In the experiment, the VLP-2000-3W laser is used as the excitation light source of near-concentric cavity A, while the PN-532-2.5W laser is used as the excitation light source of near-concentric cavity B. Five concave mirrors (M_1, M_2, M_3, M_4, and M_5) are with a diameter of 25.4 mm and a reflectivity of more than 99.5% at 532 nm. The near-concentric cavity A is composed of two concave mirrors, M_1 and M_2 ($f = -20$ mm). The near-concentric cavity B is composed of two concave mirrors, M_3 and M_4 ($f = -25$ mm). An SR-500i-B1 spectrometer produced by Andor Company with a grating notch density of 1200 mm^{-1}, blaze wavelength of 500 nm, and incident slit of 200 μm, is used. The detector uses the DR-316B-LDC-DD scientific charge-coupled device (CCD) camera of the Andor Company. The operating temperature is −60°C. The resultant spectral range is 1200–2400 cm^{-1}. The integration time of the CCD is set to 10 s, with a cumulative count of 10 times. To verify the repeatability of the experiment results, 10 sets of data were collected at each power group.
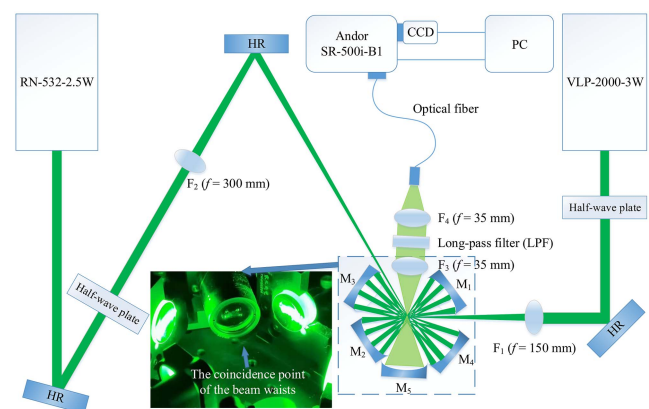

Fig. 1. The luminous distribution of near-concentric cavities and DNCCG. (a) Near-concentric cavity A; (b) near-concentric cavity B; (c) DNCCG. The different colors represent the different ray energies: 100% ≥ red > 66.6%; 66.6% ≥ green > 33.3%; 33.3% ≥ blue > 0.

Fig. 2. Device diagram of the gas Raman spectroscopy system of DNCCG.

The laser emitted by the VLP-2000-3W laser is reflected by the total mirror through the half-wave plate. It then enters the near-concentric cavity A after passing through the lens F_1. The signal emitted by the RN-532-2.5W laser is reflected by the total mirror, through the half-wave plate and lens F_2, and then reflected by the total mirror into the near-concentric cavity B. In the present experiment, to form a DNCCG, we adjust the two near-concentric cavities so that the beam waists generated by the lasers in the two near-concentric cavities coincide (i.e., when VLP-2000-3W and PN-532-2.5W lasers are simultaneously turned on) (see Fig. 2). The Raman signal generated by multiple reflections of the laser in the cavity and converging at the center of the optical cavity is coupled into the optical fiber after being collimated by the double-glued lens F_3 and focused by F_4, and finally introduced into the spectrometer for spectroscopic detection. In order to eliminate the influence of the excitation light on the Raman signal, a 532 nm LPF is added in the middle of the lens group. The addition of concave mirror M_5 ($f = -25$ mm) can further improve the efficiency of signal collection. The experimental system built in this study belongs to an open cavity. The system is placed in the measured gas to measure it. Additionally, more detailed information on the parameters and functionalities of different optical components can be found in Table S1 (Supplementary Material).

3. Results and Discussion

3.1. Comparison of simulation results between near-concentric cavities and DNCCG

According to Fig. 1, the reflection times of laser 1 in the near-concentric cavity A were 75, and the luminous flux at the beam waist was 19.56 W. The number of reflections of laser 2 in the near-concentric cavity B was 62, and the luminous flux at the beam waist was 35.80 W. The total number of reflections of laser 1 and laser 2 in the DNCCG was 138, and the luminous flux at the beam waists' coincidence point was 55.47 W.

Based on the simulation results, we found that DNCCG increased the reflection times of laser 1 in near-concentric cavity A by one unit, thus resulting in the luminous flux at the beam waist of near-concentric cavity A being increased to 19.67 W. In addition, the reflection times of laser 2 in near-concentric cavity B did not change in DNCCG. These shifts in DNCCG lead to a larger number of reflections, which further increased the luminous flux at the beam waists' coincidence point, compared with the sum of the two nonsuperposed near-concentric cavities. Compared to the near-concentric cavity proposed by Yang et al.[20], the DNCCG developed in our study significantly enhanced the ray density and the luminous flux at the beam waists' coincidence point. Altogether, these discussions suggest that such ray distribution is conducive to the enhancement of Raman signals, which could more accurately detect the Raman signals. Therefore, one of the most critical future research priorities should focus on further optimizing the structure of multiple reflection cavities, which could enhance the ray density and the luminous flux of the optical cavity.

3.2. Comparison of the Raman signal intensity between near-concentric cavities and DNCCG

To further verify the simulation results and explore the practical performance of DNCCG, we conducted the experiment with air as a sample in our lab. According to Fig. 3, O_2 and N_2 Raman signals were located at 1555 cm^{-1} and 2330 cm^{-1}, respectively.
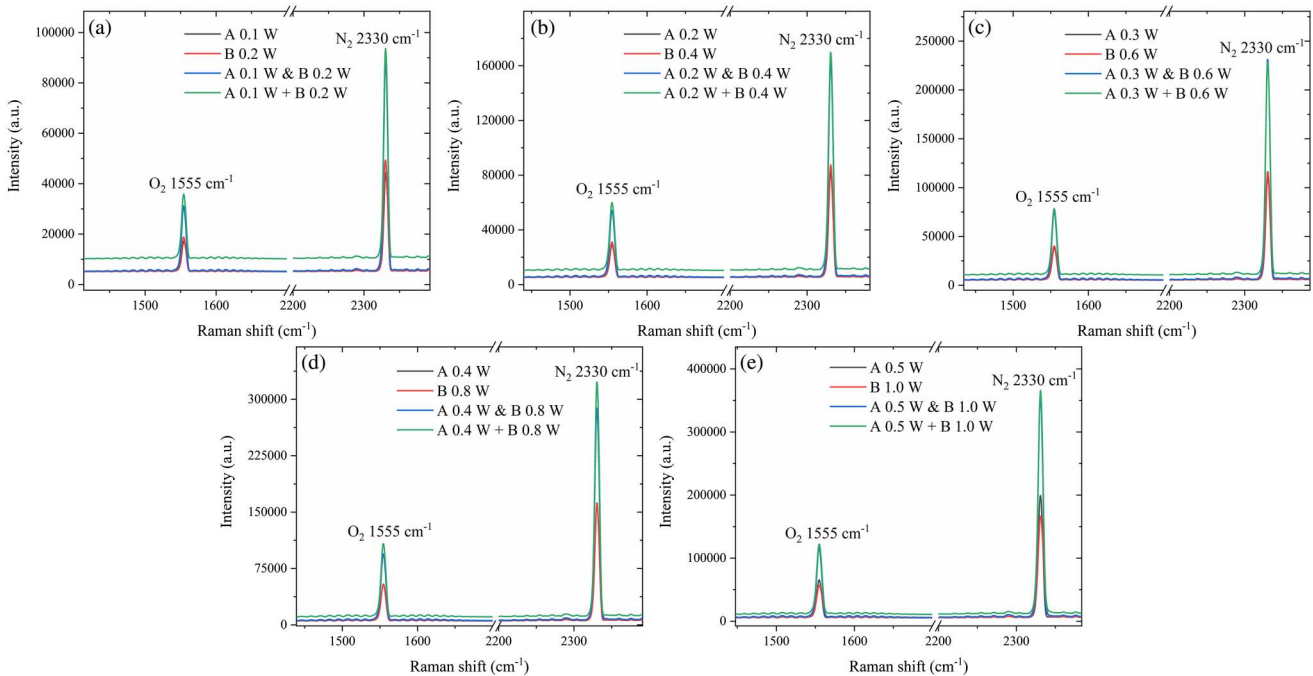

Fig. 3. Comparison of Raman spectra of DNCCG (A & B), near-concentric cavities (A, B), and the sum of two near-concentric cavities (A + B).

The background noise of DNCCG is about half of the sum of the background intensity of two near-concentric cavities under different incident beam powers. Therefore, compared with the near-concentric cavities, superimposing two near-concentric cavities to form DNCCG can increase the signal-to-background ratio (SBR), which is beneficial in improving the Raman signal intensity. In addition, to further compare the signal intensity between DNCCG and the sum of two near-concentric cavities, the present study selected the average intensity in the range of 2000–2100 cm^{-1} as a baseline and took the Raman peak after removing the baseline as the signal intensity.

According to Fig. 4, the results showed that compared with the sum of two near-concentric cavities, DNCCG had a stronger CO_2 Raman signal intensity at the signal collection [Fig. 4(a), inset]. This further verified the previous simulation results: DNCCG had a larger number of reflections and luminous flux compared to the sum of the two near-concentric cavities. Two reasons might explain this gain. First of all, DNCCG is realized by using two lasers plus two multiple reflection cavities, and its essence is the superposition of two cavity signals. When two lasers in the system are switched on at the same time, two near-concentric cavities are superimposed to form a DNCCG. Therefore, compared with one of the near-concentric cavities, the DNCCG could improve the total power of the incident beam. Similarly, Li *et al.*[16] also used low-power laser sources to achieve external cavity power amplification. However, the experimental results also found that DNCCG did not have a stronger CO_2 Raman signal intensity in the case of A 0.1 W and B 0.2 W [Fig. 4(a), inset]. This indicates that there probably exists a power threshold. The power threshold could be attributed to the increase in background noise caused by CCD noise having a greater impact on the Raman signal intensity due to the lower baseline under low-power conditions (i.e., the case of power A 0.1 W and B 0.2 W), compared to the high-power conditions. Specifically, in experimental spectrum collection, CCD noises are the primary source of instrument noise (i.e., photon shot noise, dark current noise, and readout noise). These CCD noises affect the collection of Raman spectra, including increasing background noise and reducing the SBR. These shifts would increase the baseline of spectra. The increase in baseline could decrease the Raman signal intensity. Under low-power conditions (the case of power A 0.1 W and B 0.2 W), due to the lower baseline, the increase in background noise caused by CCD noise has a greater impact on the Raman signal intensity when compared to other high-power conditions. This leads to uncertainty in the increase of CO_2 Raman signal strength at low-power conditions, thus producing a power threshold. We will try to use a low-noise CCD in future studies to further improve the gain of DNCCG on gas Raman signals in the low-power condition, so that the experimental results can better match the simulated results.

Meanwhile, DNCCG improves the ray density of the cavity center through the superposition of two near-concentric cavities, which further enhances the luminous flux. Moreover, the present study found that compared with the two near-concentric cavities, DNCCG not only has higher light density and luminous flux in the center of the optical cavity, but also has more reflection times of incident light and larger optical path length. Such higher light density, luminous flux, reflection times, and optical path length enable DNCCG to increase
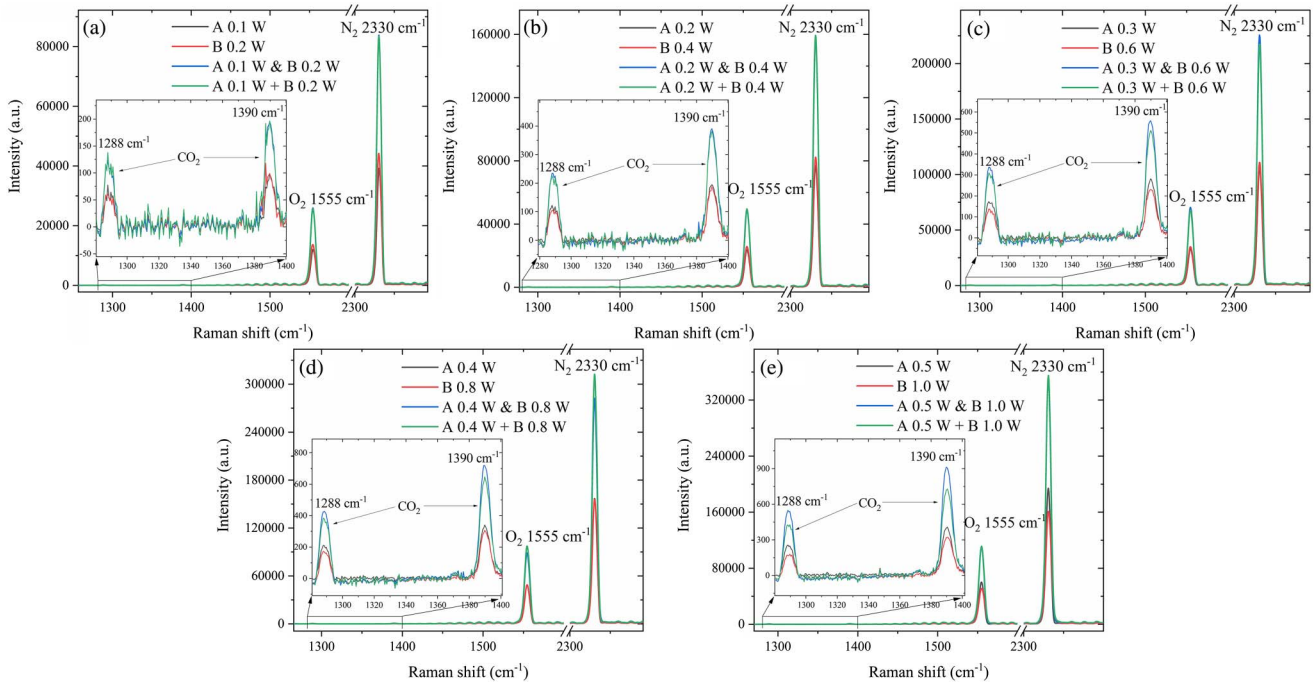

Fig. 4. Comparison of the Raman signal intensity of DNCCG (A & B), near-concentric cavities (A, B), and the sum of the two near-concentric cavities (A + B).

Raman signal intensity by 1.9–2.1 and 2.3–2.5 times, respectively, compared to two near-concentric cavities. These gains are higher than those in previous technologies. For example, Liu et al.[21] also developed a folded near-concentric cavity based on near-concentric cavity improvement technology. This technique improves the light density and luminous flux without increasing the reflection times of incident light. Thus, it only increases the Raman signal intensity by 1.5 times. Such ray distribution is more conducive to the detection of Raman signals. More importantly, DNCCG can improve the Raman signal intensity by attenuating the increase in background intensity. Consequently, DNCCG can improve the Raman signal intensity by increasing the total incident light power and weakening the increase of background intensity. Therefore, future research can optimize the new technologies in these two aspects to achieve further enhancement of Raman signals.

To further quantify the enhancement effect of DNCCG on Raman signal intensity and SNR, we calculated the Raman signal intensity, noise intensity, SNR, and change in signal intensity (Table S2 in Supplementary Material). To calculate the noise intensity, we selected the RMS noise level in the range of 2000–2100 cm^{-1} of the spectrum as the spectral noise standard. In addition, the CO_2 Raman signal values after removing the baseline were used as the signal intensity.

The results showed that compared with near-concentric cavity A and near-concentric cavity B, DNCCG increased the SNR of the CO_2 Raman signal at 1288 cm^{-1} by 2.0 and 2.4 times, respectively. And the corresponding increases in the SNR at 1390 cm^{-1} were 2.1 and 2.3 times, respectively. This suggests that DNCCG has a significant enhancement effect on the SNR of the CO_2 signal.

The positive effect of DNCCG on SNR can be explained in two ways. On the one hand, DNCCG enhanced the Raman signal intensity. Specifically, compared to near-concentric cavity A and near-concentric cavity B, DNCCG increased the CO_2 Raman signal intensity at 1288 cm^{-1} by 1.9 and 2.5 times, respectively, and the corresponding increases at 1390 cm^{-1} were 2.1 and 2.3 times, respectively. Notably, compared with the sum of two near-concentric cavities, DNCCG also increased the Raman signal intensity of CO_2 by about 10% on average, at 1288 cm^{-1} and 1390 cm^{-1}. In addition, we found that the difference in CO_2 Raman signal intensity between DNCCG and the sum of two near-concentric cavities increased with power. The SNR of CO_2 Raman signals was enhanced with the increase of incident light power, and there is a significantly linear relationship between the SNR and the incident light power, $R^2 = 0.986$ (see Fig. 5). On the other hand, there was no significant ($P > 0.05$) change detected on either Δ noise intensity A or Δ noise intensity B (see Fig. 6). Subsequently, we obtained the unexpected result that the noise intensity of DNCCG was not enhanced by the superposition of the near-concentric cavities. Thus, we conclude that DNCCG improves the Raman signal intensity without affecting the noise intensity, which improves the SNR and enhances the detection sensitivity.
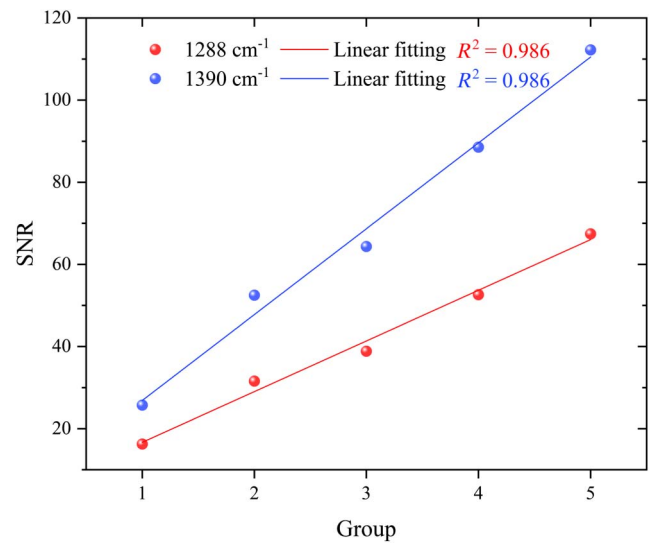

Fig. 5. Scatterplots for SNR of CO_2 Raman signals in different groups. The incident light power is increased with the group number (Table S2 in Supplementary Material).

Fig. 6. Scatterplots for Δ noise intensity of CO_2 Raman signals in different groups. The incident light power is increased with the group number (Table S2 in Supplementary Material). Δ noise intensity A, B = noise intensity A & B - noise intensity A, B.
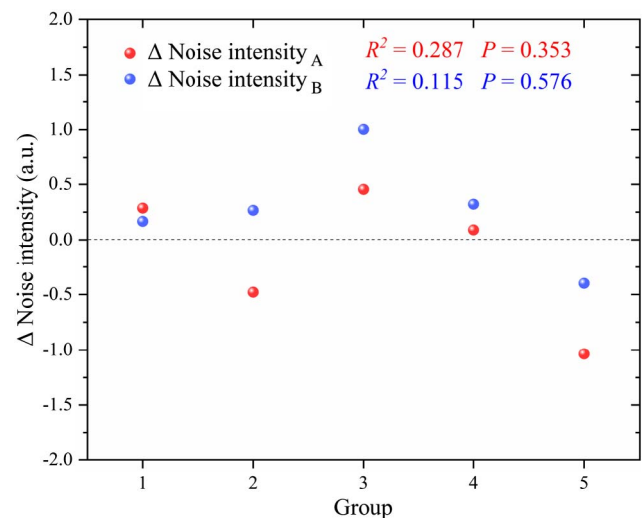
It should be noted that the gas medium has the characteristics of a small scattering cross section and relatively low molecular density, which might result in low Raman signal intensity. To further enhance the signal intensity of DNCCG, future research can further increase the gas Raman signal intensity by compressing the gas medium to increase the molecular density. For example, a gas sample cell with high collection efficiency could be installed at the signal collection point to compress the measured gas, which can further enhance the gas Raman signal intensity and improve its SNR.

3.3. LOD of CO_2 by the gas Raman spectroscopy system of DNCCG

In the present study, to estimate the LOD of DNCCG, we used air as the measured gas and adjusted the laser power of VLP-2000-3W and PN-532-2.5W lasers to the maximum. The Raman signal intensity of CO_2 (1390 cm^{-1}) is 1182.4 (a.u.), and the noise intensity is 10.6 (a.u.) at the maximum power. In addition, considering that the concentrations of CO_2 in the laboratory are usually higher than that in the atmosphere, the CO_2 concentration in the laboratory should be estimated as 916 ppm, which could more accurately estimate the LOD of DNCCG. Because the LOD standard is 3 times the noise intensity, the LOD of CO_2 in the DNCCG Raman spectroscopy system is 24.6 ppm.

Altogether, these results collectively suggest that DNCCG can significantly reduce the LOD and increase the detection sensitivity, which could effectively improve the detection ability of trace gases.

4. Conclusion

The present study proposed a DNCCG to measure the gas Raman spectroscopy. The effectiveness of DNCCG was verified by TracePro software simulation and systematic experiments. The simulation results showed that DNCCG significantly enhanced the luminous flux of the laser at the coincidence point of the beam waists. The systematic experiments found that DNCCG enhanced the Raman signal intensity by increasing the total incident light power and weakening the increase of background intensity. Moreover, DNCCG did not significantly affect the noise intensity. Thus, DNCCG effectively improved the SNR. Importantly, we estimated that the LOD of DNCCG for CO_2 was as low as 24.6 ppm. Consequently, our results highlight that DNCCG can be an effective and promising method to enhance trace gas detection sensitivity and obtain an extensive dynamic detection range. To broaden the application of this method, future research could combine DNCCG with an airtight gas sample cell for the detection of some more different gases.

Acknowledgements

References

1. R. E. Dickinson and R. J. Cicerone, "Future global warming from atmospheric trace gases," Nature **319**, 109 (1986).
2. L. Zhang, H. Y. Zheng, Y. P. Wang, *et al.*, "Characteristics of Raman spectrum from stand-off detection," Acta Phys. Sin. **65**, 054206 (2016).
3. W. Zhang, Y. Tang, A. Shi, *et al.*, "Recent developments in spectroscopic techniques for the detection of explosives," Materials **11**, 1364 (2018).
4. Y. Gao, L.-K. Dai, H.-D. Zhu, *et al.*, "Quantitative analysis of main components of natural gas based on Raman spectroscopy," Chin. J. Anal. Chem. **47**, 67 (2019).
5. J. Wang, P. Wang, W. Chen, *et al.*, "Highly sensitive multi-pass cavity enhanced Raman spectroscopy with novel polarization filtering for quantitative measurement of SF_6 decomposed components in gas-insulated power equipment," Sens. Actuators B Chem. **380**, 133350 (2023).
6. H. Kim, A. Zubairova, M. Aldén, *et al.*, "Signal-enhanced Raman spectroscopy with a multi-pass cavity for quantitative measurements of formaldehyde, major species and temperature in a one-dimensional laminar DME-air flame," Combust. Flame **244**, 112221 (2022).
7. P. Wang, W. Chen, J. Wang, *et al.*, "Hazardous gas detection by cavity-enhanced Raman spectroscopy for environmental safety monitoring," Anal. Chem. **93**, 15474 (2021).
8. P. Wang, W. Chen, J. Wang, *et al.*, "Dense-pattern multi-pass cavity based on spherical mirrors in a Z-shaped configuration for Raman gas sensing," Opt. Lett. **47**, 2466 (2022).
9. S. Schlüter, F. Krischke, N. Popovska-Leipertz, *et al.*, "Demonstration of a signal enhanced fast Raman sensor for multi-species gas analyses at a low pressure range for anesthesia monitoring," J. Raman Spectrosc. **46**, 708 (2015).
10. D. V. Petrov, "Multipass optical system for a Raman gas spectrometer," Appl. Opt. **55**, 9521 (2016).
11. A. P. Shreve, N. J. Cherepy, and R. A. Mathies, "Effective rejection of fluorescence interference in Raman spectroscopy using a shifted excitation difference technique," Appl. Spectrosc. **46**, 707 (1992).
12. X. Liu and Y. Ma, "Sensitive carbon monoxide detection based on light-induced thermoelastic spectroscopy with a fiber-coupled multipass cell," Chin. Opt. Lett. **20**, 031201 (2022).
13. J. Gomez Velez and A. Muller, "Trace gas sensing using diode-pumped collinearly detected spontaneous Raman scattering enhanced by a multipass cell," Opt. Lett. **45**, 133 (2020).
14. X. Li, Y. Xia, L. Zhan, *et al.*, "Near-confocal cavity-enhanced Raman spectroscopy for multitrace-gas detection," Opt. Lett. **33**, 2143 (2008).
15. G. A. Waldherr and H. Lin, "Gain analysis of an optical multipass cell for spectroscopic measurements in luminous environments," Appl. Opt. **47**, 901 (2008).
16. B. Li, S.-W. Luo, A.-L. Yu, *et al.*, "Confocal-cavity-enhanced Raman scattering of ambient air," Acta Phys. Sin. **66**, 190703 (2017).
17. R. A. Hill and D. L. Hartley, "Focused, multiple-pass cell for Raman scattering," Appl. Opt. **13**, 186 (1974).
18. K. C. Utsav, J. A. Silver, D. C. Hovde, *et al.*, "Improved multiple-pass Raman spectrometer," Appl. Opt. **50**, 4805 (2011).
19. W. R. Trutna and R. L. Byer, "Multiple-pass Raman gain cell," Appl. Opt. **19**, 301 (1980).
20. D. Yang, J. Guo, Z. Du, *et al.*, "Raman signal enhancement for gas detection using a near concentric cavity," Spectrosc. Spect. Anal. **35**, 645 (2015).
21. Q.-S. Liu, D.-W. Yang, J.-J. Guo, *et al.*, "Raman spectroscopy for gas detection using a folded near-concentric cavity," Spectrosc. Spect. Anal. **40**, 3390 (2020).